



The methylation inhibitor 3DZNep promotes HDR pathway choice during CRISPR-Cas9 genome editing



Nadja Bischoff^a, Sandra Wimberger^b, Ralf Kühn^c, Anne Laugesen^a, Volkan Turan^a,
Brian Daniel Larsen^a, Claus Storgaard Sørensen^a, Kristian Helin^{a,1}, Eric Paul Bennett^{d,e},
Marcello Maresca^b, Cord Brakebusch^{a,*}

^a Biotech Research and Innovation Center (BRIC), University of Copenhagen, Ole Maaløes Vej 5, Copenhagen 2200, Denmark

^b Discovery Sciences, BioPharmaceuticals R&D, AstraZeneca, Pepparedsleden 1, 43 183 Mölndal, Gothenburg, Sweden

^c Max Delbrück Center for Molecular Medicine, Robert-Rössle-Str. 10, Berlin 13125, Germany

^d Department of Odontology and Molecular and Cellular Medicine, Copenhagen Center for Glycomics, Faculty of Health Sciences, University of Copenhagen, Copenhagen N 2200, Denmark

^e RNA & Gene Therapies, Gene Editing Department, Novo Nordisk, Novo Nordisk Park, Måløv 2760, Denmark

ARTICLE INFO

Keywords:

CRISPR-Cas9
Histone methylation
Chromatin modification
HDR
NHEJ

ABSTRACT

Alteration of specific epigenetic marks might promote homology directed repair (HDR) during CRISPR-Cas9 genome editing. Testing several epigenetic inhibitors in a traffic light reporter assay, the histone methylation inhibitor 3DZNep showed a significant HDR promoting effect, while non-homologous end joining mediated repair was not significantly changed. This HDR promoting effect was largely independent of the target gene and its expression levels but showed a limited cell type specificity. HDR promotion was independent of the best described target of 3DZNep, the H3K27 methyltransferase EZH2, and of altered gene expression, but correlated partially with increased frequency of S/G2 cell cycle stage.

1. Introduction

Defined CRISPR-Cas9 genome editing by homology directed repair (HDR) is important for the introduction of point mutations and DNA donor constructs into cell lines, animals, and for the therapy of human genetic diseases. However, efficiency of DNA double-strand break (DSB) repair by HDR is in general much lower than of the unwanted, competitive repair by non-homologous end joining (NHEJ). It is therefore of high interest to find simple procedures which twist the DSB repair pathway choice during CRISPR-Cas9 genome editing towards HDR without reducing total genome editing efficiency [1]. Genome editing efficiency is influenced by the cutting efficiency of sgRNA/Cas9, the expression of proteins involved in DNA repair, and by their recruitment to the DSB. Chromatin modifications are suggested to regulate all these processes. Inhibition of DNA methylation by 5-azacytidine (5-aza) was not found to alter genome editing efficiency in a semiquantitative assay [2]. Histone 3 lysine 36 trimethylation (H3K36me3) promoted HDR, while H3K36me2 increased NHEJ in a context dependent manner [3,4]. Dense DNA packing in heterochromatin, which is characterized by H3K27me3 and H3K9me3, was reported to influence the speed of repair at low concentrations of CRISPR-Cas9, but not the HDR/NHEJ pathway choice [5].

In another experimental system, it was found to affect NHEJ efficiency, but less HDR efficiency [6]. However, a spike of H3K9me3 was reported to be required for HDR and pre-existing H3K9me3 was shown to reduce HDR [7]. H4K20 methylation was suggested to favor NHEJ [8]. Finally, inhibition of histone deacetylation was found to increase both NHEJ and HDR [9]. Taken together, chromatin modifications appear to influence the efficiency and pathway choice of DSB repair, although the underlying molecular mechanisms are poorly characterized. Small molecule inhibitors of chromatin modifying enzymes might therefore be useful to promote HDR in CRISPR-Cas9 genome editing. However, no such inhibitor is currently used routinely for that purpose.

In this study we investigated the influence of a set of small molecule inhibitors of chromatin modification on CRISPR-Cas9 genome editing. We identify 3DZNep, which inhibits the H3K27 methyltransferase EZH2 and methylations dependent on S-adenosylhomocystein [10,11], as a novel promoter of HDR dependent CRISPR-Cas9 genome editing. Surprisingly, this effect was independent from EZH2 and correlated only partially with alterations of the cell cycle. As 3DZNep improved HDR efficiency of different target genes in different cell types to up to 80%, while in most cases reducing error-prone NHEJ repair, it might be a simple method to improve defined genome editing efficiency.

* Corresponding author.

E-mail address: cord.brakebusch@bric.ku.dk (C. Brakebusch).

¹ Present address: The Institute of Cancer Research, 237 Fulham Road, London SW3 6JB, United Kingdom.

2. Material and methods

2.1. Cell lines

HEK293/TLR, HEK293T, U2OS or N2A cells were kept in DMEM/GlutaMAX (GIBCO) supplemented with 10% FBS (Hyclone) and 1% penicillin-streptomycin (GIBCO). Mouse embryonic stem (mES) cells were kept on gelatin-coated dishes in 2i/LIF-containing medium [12]. All cells were kept in a humidified 37 °C incubator with 5% CO₂.

2.2. Transfections

0.5 × 10⁶ HEK293/TLR or HEK293T cells were seeded in 6-well dishes one day prior transfection and transfected with 2 µg total DNA and 8 µl 1 mg/ml linear PEI solution (pH 7.0; Polysciences) in 200 µl Opti-MEM (Invitrogen), which was incubated at room temperature for 30 min and then added dropwise to cells. 0.5 × 10⁶ N2A or 0.3 × 10⁶ U2OS cells were seeded in 6-well plates and transfected the following day with GeneJet transfection medium (SigmaGen) according to manufacturer's instructions. 1.6 × 10⁶ mES cells were seeded in 10 cm dishes and at the same time transfected with Lipofectamine 3000 medium (ThermoFisher) according to manufacturer's instructions.

2.3. Inhibitor treatment

Inhibitor treatment was performed for 24 h (cell cycle analysis) or 48 h (CRISPR-Cas9 editing) with 50 µM Am1, 5 or 10 µM BRD4770, 2 µM BIX01294, 0.5 µM 3-Deazaneplanocin (3DZNep), 5 or 10 µM GSK-J4, 100 µM IOX-1, 2 µM Tranylcypromine hydrochloride (2-PCPA), 0.5 or 5 µM 5-azacytidine (5-aza), 1 µM Trichostatin A (TSA), 20 or 50 µM C646 (all Tocris), 1 µM EPZ-643 (MedChemExpress), 0.5 µM UNC-0379, 10 µM A196 or DMSO (all Sigma).

2.4. Western blot analysis

Inhibitor treated cells were harvested, washed with PBS, and the cell pellets snap frozen and stored at -80°C. Cell pellets were thawed in TOPEX+ buffer with protease inhibitors [13]. SDS-PAGE and Western blotting, and ECL were carried out according to standard protocols. The following primary antibodies were used: Histone H4 (Merck #07-108, 1:10.000), H3K27me3 (Cell Signalling, #9733, 1:1000), H3K9me2 (Cell Signalling, #4658, 1:1000), H3K4me2 (Cell Signalling, #9725, 1:1000), EZH2 (BD43, Helin lab, 1:10), Lamin B1 (Abcam #16048, 1:10.000), GAPDH (Merck, #G9545, 1:10 000). As secondary antibodies, Horseradish peroxidase (HRP)-coupled horse anti-mouse IgG (Vector, PI-2000) or goat anti-rabbit IgG (Vector, PI-1000) were used (1:10.000).

2.5. Design of sgRNAs, primers and ssODNs

sgRNAs were designed with CRISPOR [14] (Supp. Table. 1A). Primers were designed using PrimerBlast [15] (Supp. Table 1C). sgRNAs and primers used for studying off-target efficiency were described earlier [16,17]. Desalted oligos were ordered from Thermo Fisher. Single-strand oligodeoxynucleotides (ssODNs), used as HDR repair template for gene editing in HEK293T, U2OS, N2A or mES cells, were designed with homology arms of 50 nt each, and an 8 nt insertion containing a HindIII restriction site (Supp. Table 1B). ssODNs were ordered as ultramers from IDT.

2.6. Plasmids and cloning

Targeting plasmids for CRISPR-Cas9 editing of *PAX2*, *L PXN*, *HOXD13*, *PHOX2B*, *TSPAN12* or *EZH2* were created by cloning sgRNAs into vectors expressing Cas9 and either a puromycin resistance (Addgene, #62988) or a GFP (Addgene, #48138) following standard techniques.

2.7. Analysis of genome editing efficiency

TLR: The HEK293/TLR system was used with HEK293 cells stably expressing Cas9 [18]. DMSO or no addition were used as controls. 48 h after transfection flow cytometry was performed on an LSR using FACS-Diva (BD) and analyzed by FlowJo software (version 10.7.1 for MacOS). Repair efficiencies and ratios were compared to control cells incubated in DMEM (Suppl. Fig. 1).

NGS: For NGS analysis, genomic DNA was amplified using the primers hPAX2_NGS_fwd and hPAX2_NGS_rev. NGS library preparation and subsequent bioinformatic analysis was performed as described previously [20] (Suppl. Fig. 2B). Variants were further analyzed with RIMA [21].

Restriction digest: Genomic PCRs were digested with HindIII and relative amounts of fragments were determined after gel electrophoresis by ImageJ.

TIDE/TIDER/ICE: TIDE/TIDER analysis of Sanger sequencing of genomic PCRs covering the target region was carried out as described [22] (Fig. 2C, D). Briefly, DNA sequences obtained from genomic PCRs after genome editing were compared to wildtype (TIDE, TIDER) and to HDR modified (TIDER) control sequences. The R² values of the TIDER and ICE analyses were always higher or equal to 0.95. For the TIDE analysis R² values ranged from 0.77 to 0.93. The software then calculated the percentage of indels and HDR in the genome edited samples. Sanger sequencing traces were additionally used for ICE analysis (<https://ice.synthego.com/#/>).

IDAA [19]: Transfected cells were sorted for GFP+ cells or, when indicated, selected by puromycin treatment (4 days with 1 -2 µg/ml) (Suppl. Fig. 2E). Sorting was performed on the BD FACS Aria III Cell sorter, including 7-AAD staining to exclude dead cells. Genomic DNA was extracted using QuickExtract (Lucigen) and used as template for tri-primer IDAA PCR reactions (Supp. Table 1C). PCR products containing fragments of different lengths depending on the editing event were then size-separated on an ABI Genetic Analyzer 3500 and analyzed by Viking ProfileIT indel profiling software (<https://viking.sdu.dk>). To exclude background, only fragments in the size range of +/-25 base pairs of the WT fragment were considered. The +8 bp fragment was considered as HDR and all other fragment different from WT as NHEJ.

2.8. Cell cycle analysis

Cell cycle analysis was performed using the Click-iT EdU Flow Cytometry Cell Proliferation Assay (ThermoFisher) and propidium iodide incubation. Flow cytometry analysis was performed on FACSCalibur using the CellQuest Pro Software (BD). Data were analyzed with FlowJo software (version 10.7.1 for Mac OS X).

2.9. EZH2 knockout

HEK293T cells were transfected with an expression vector for an EZH2 targeting sgRNA, Cas9 and GFP. 48 h after transfection GFP+ single cells were sorted into 96 well plates containing conditioned media. An EZH2 KO clone was identified by IDAA and confirmed by Western Blot analysis for a truncated EZH2 protein and lack of H3K27me3.

2.10. RNAseq analysis

HEK293T or mES cells were incubated in 0.5 µM 3DZNep for 24 h and then detached, pelleted and snap frozen. RNA extraction, polyA selection, strand specific sequencing and downstream data analysis was performed by Genewiz using the DESeq2 program, which provides a readout of "normalised counts" by normalizing to the geometric mean of counts over all samples for each gene [23]. Genes were functionally annotated by DAVID [24].

2.11. Statistical analysis

Bar graphs present mean values of at least three biological replicates, with error bars showing standard deviation (SD). Statistical significance was determined by unpaired *t*-test, multiple *t*-test (with post-hoc Holm-Sidak correction), 1-way ANOVA or 2-way ANOVA (with post-hoc Dunnett’s correction). Statistical analysis was performed in R-Studio (version 1.3.1093) or Prism 8 (version 8.4.3). Significant differences are indicated by asterisks (**p* ≤ 0.05; ***p* ≤ 0.01; ****p* ≤ 0.001; *****p* ≤ 0.0001).

3. Results

3.1. 3DZNep promotes HDR pathway choice during CRISPR-Cas9 genome editing in HEK293/TLR cells

To test the role of chromatin modifications on genome editing we applied 10 different small molecule inhibitors for histone methyltransferases (HMT), histone demethylases (HDM), histone acetyltransferases (HAT), histone deacetylases (HDAC), or DNA methyltransferases (DNMT) (Supp. Table 2) in a reporter system where Cas9 expressing HEK293/TLR cells were transfected with an sgRNA expressing plasmid and a dsDNA donor template. Among the blue fluorescent transfected cells, HDR events were recognized by Venus fluorescence and NHEJ dependent 2 bp frameshifts by RFP fluorescence using flow cytometry 2d after transfection. A significant HDR promoting effect was identified for 3DZNep, while NHEJ was not altered (Fig. 1). The HMT inhibitors AMI1 and BIX1294 and the HDM inhibitor 2-PCPA showed neither an effect on HDR nor on NHEJ under the conditions tested. All other inhibitors impaired both HDR and NHEJ. Interestingly, high concentrations of the HAT inhibitor C646 or the DNMT inhibitor 5-aza inhibited NHEJ more than HDR, resulting in a significantly increased HDR to NHEJ ratio. These data suggest that chromatin modifications can strongly influence gene targeting efficiency and DSB repair pathway choice and that 3DZNep specifically improves HDR with a dsDNA donor template.

3.2. 3DZNep promotes HDR for different target genes in HEK293T cells

To explore whether an HDR promoting effect of 3DZNep can also be observed when using an ssDNA donor template, we induced a DSB in HEK293T cells by transfection of Cas9 and sgRNA in the presence of a ssDNA donor oligonucleotide. Moreover, we investigated repair efficiency in five different target genes to explore gene-to-gene variation. Two of these genes were highly expressed (*HOXD13*, *TSPAN12*) and three lowly (*LPXN*, *PAX2*, *PHOX2B*) as confirmed by RNAseq analysis (Supp. Table 3). As donor template an ssODN was used which inserted 8 bp containing a HindIII restriction site by HDR, similar to other reports [25]. It should, however, be noted that the mode of action for ssODN-directed CRISPR gene editing is still under discussion with synthesis-dependent strand annealing (SDSA) or Excision and Corrective Therapy (ExACT) as possible alternatives [26]. Although we stick in the following to the term “HDR” this ambiguity needs to be considered for all genome editing data presented.

HDR and NHEJ events were quantified by IDAA, which was found to be comparable in respect to variation to the more expensive NGS analysis and demonstrated less variation than analysis by restriction digest or Sanger sequencing followed by TIDER or ICE (Supp. Fig. 3). For 4 target genes 3DZNep increased HDR efficiency significantly and decreased NHEJ to a similar extent, resulting in an 30–60% increase in HDR and an unchanged total editing efficiency (Fig. 2). We noted that 3DZNep treatment did not change the pattern of NHEJ repair (Supp. Fig. 4). Interestingly, differences in HDR efficiency did not correlate with the expression level of the target gene before or after 3DZNep treatment in HEK293T (Supp. Table 3).

NGS analysis allowed furthermore to distinguish microhomology-based end joining (c-MMEJ) from other c-NHEJ mediated editing events.

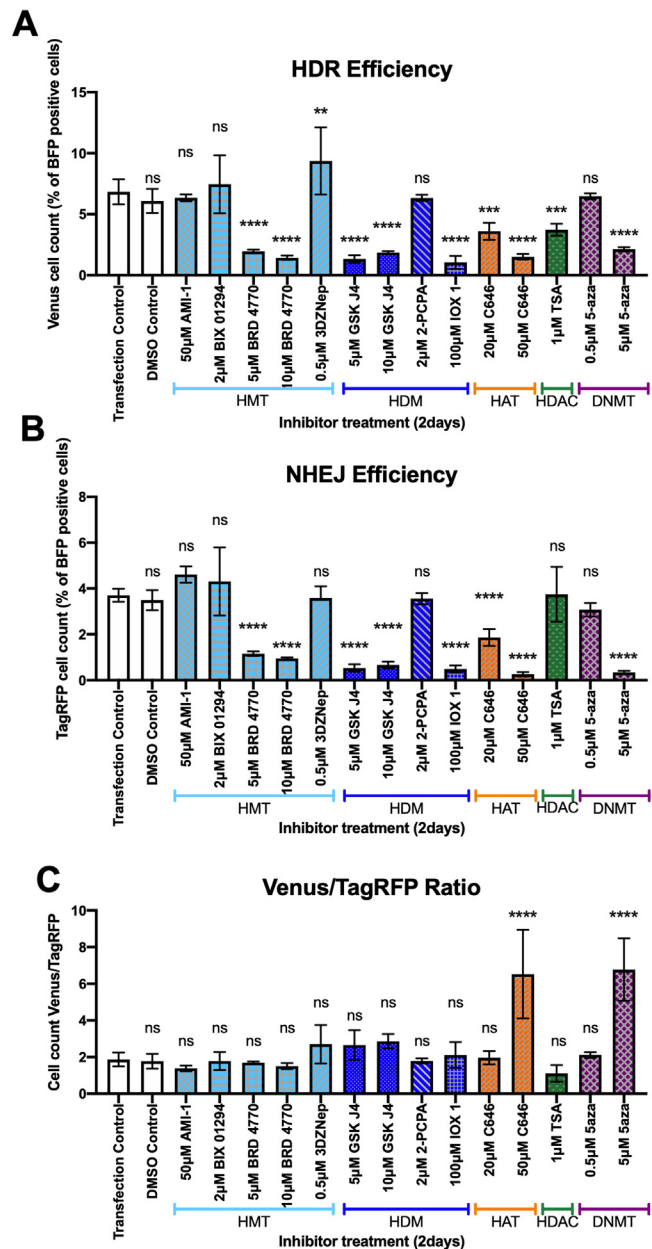


Fig. 1. Epigenetic inhibitors influence DSB repair in HEK293/TLR cells. DSB repair pathway choice was determined using the HEK293/TLR system in the presence of the indicated inhibitors of chromatin modification. (A) HDR efficiency as detected by green fluorescence, (B) NHEJ efficiency estimated by red fluorescence, (C) Ratio of HDR to estimated NHEJ efficiency. (Histone methyltransferases (HMTs), histone demethylases (HDMs), histone acetyltransferases (HATs), histone deacetylases (HDACs), DNA methyltransferases (DNMTs); *n* ≥ 3; mean with standard deviation; ANOVA; **p* ≤ 0.05; ***p* ≤ 0.01; ****p* ≤ 0.001; *****p* ≤ 0.0001; ANOVA).

c-MMEJ, defined as deletions larger or equal to 2 bp surrounded by microhomologies, was significantly reduced by 3DZNep compared to DMSO treated controls (Suppl. Fig. 5). Also, 1-bp insertion and deletions, which are very often attributed to c-NHEJ, are significantly reduced by 3DZNep, suggesting that both c-MMEJ and c-NHEJ are affected by 3DZNep. Other-EJ, defined as all mutations that are not classified as c-MMEJ or HDR, showed a reduced trend in the presence of 3DZNep that was not significant. Total editing efficiency was not significantly altered.

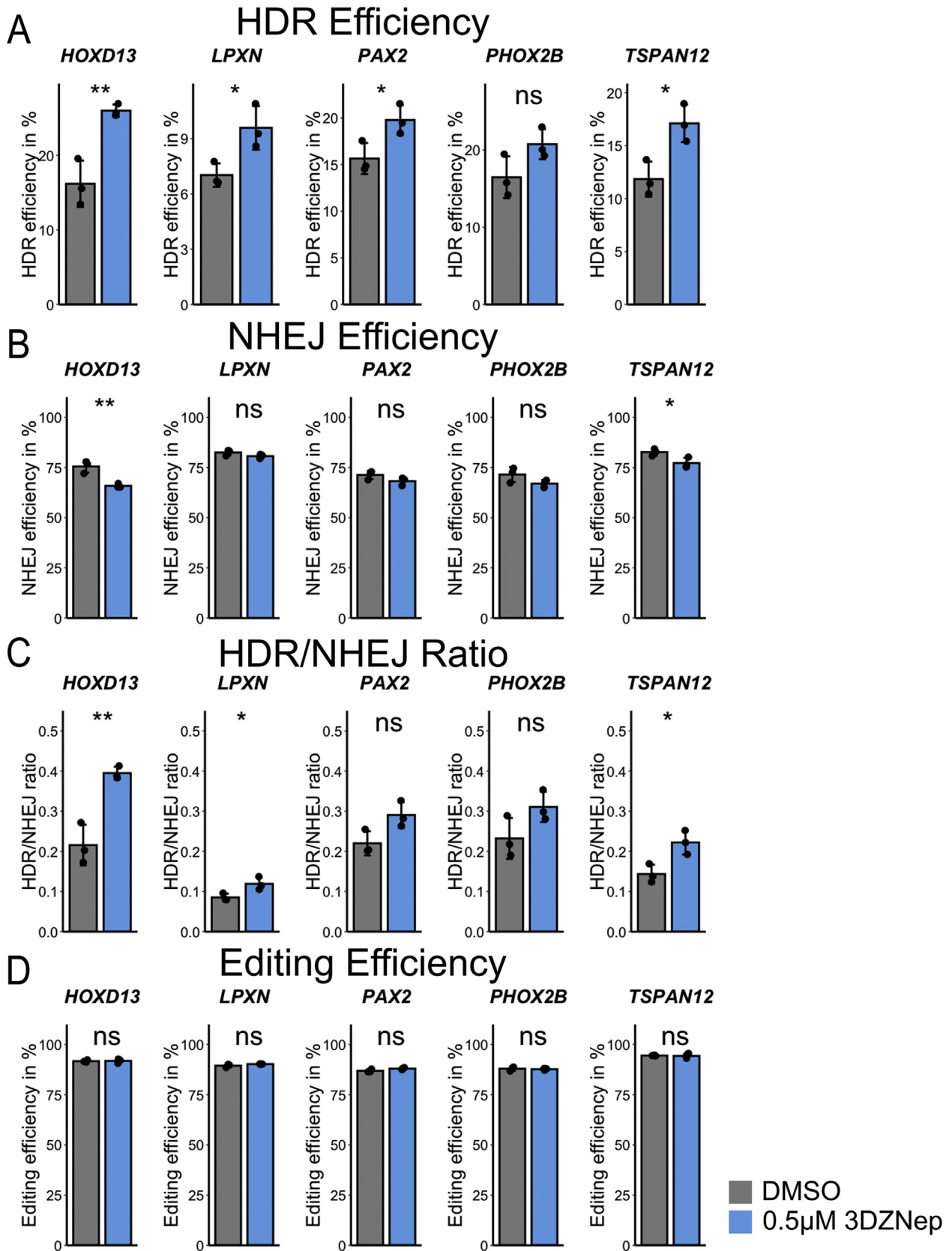


Fig. 2. 3DZnep promoted HDR pathway choice in CRISPR-Cas9 genome editing in HEK293T cells. DSB repair pathway choice was determined using the IDAA system in the presence of 0.5mM 3DZnep. (A) HDR efficiency, (B) NHEJ efficiency, (C) HDR/NHEJ ratio, (D) total editing efficiency ($n = 3$; mean with standard deviation; t -test; * : $p \leq 0.05$; ** : $p \leq 0.01$; ns : $p > 0.05$).

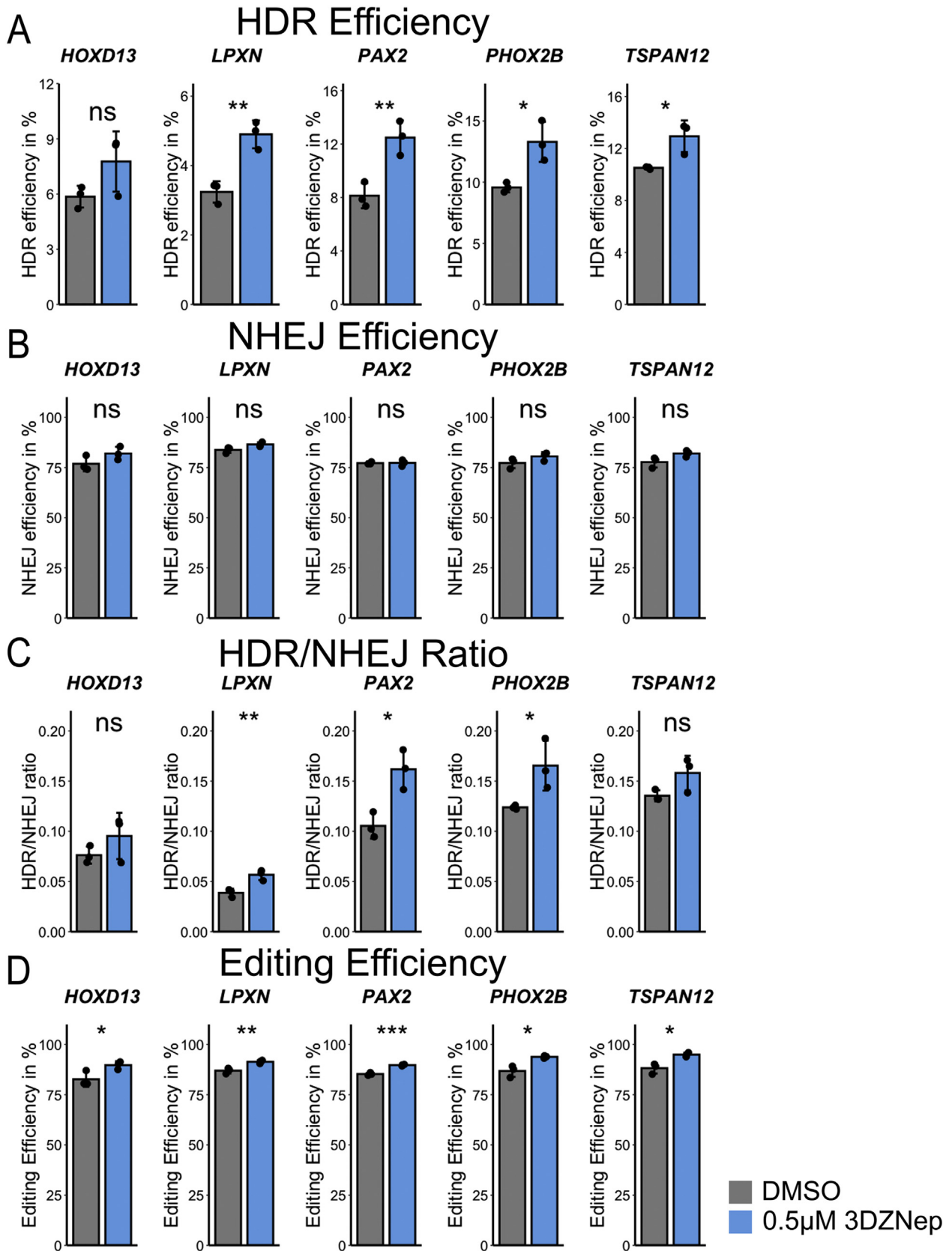


Fig. 3. 3DZNe promoted HDR pathway choice in CRISPR-Cas9 genome editing in U2OS cells. DSB repair pathway choice was determined using the IDAA system in the presence of 0.5mM 3DZNe. Transfected cells were selected by puromycin. (A) HDR efficiency, (B) NHEJ efficiency, (C) HDR/NHEJ ratio, (D) total editing efficiency ($n = 3$; mean with standard deviation; t -test; * : $p \leq 0.05$; ** : $p \leq 0.01$; *** : $p \leq 0.001$; ns : $p > 0.05$).

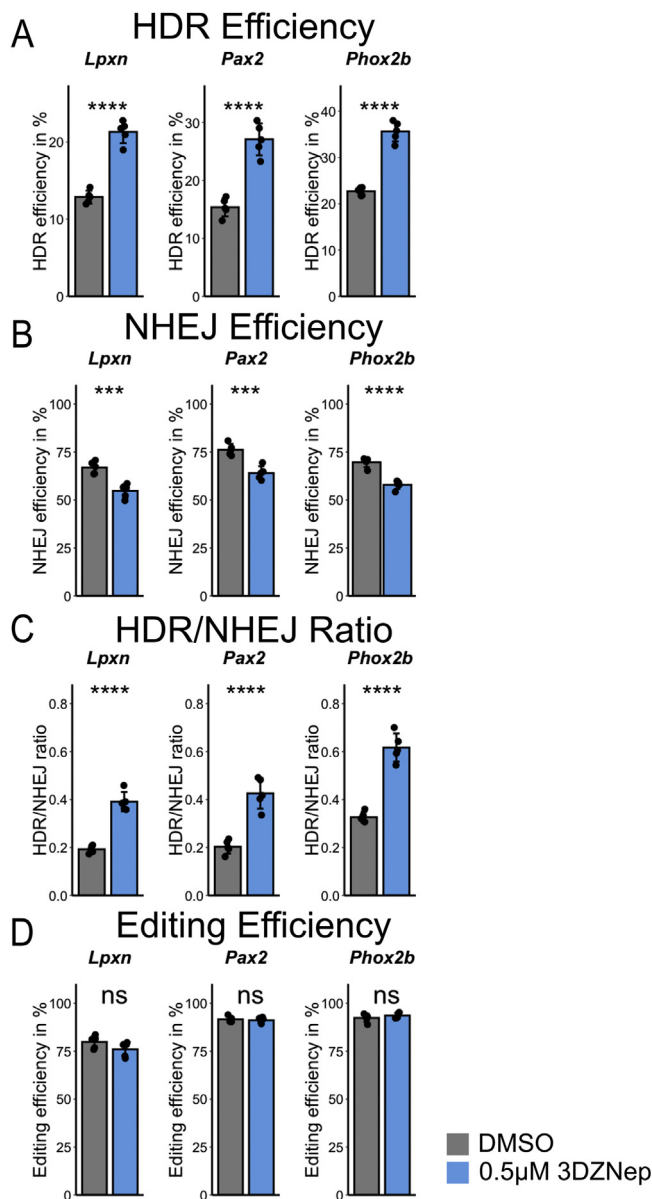


Fig. 4. 3DZnep promoted HDR pathway choice in CRISPR-Cas9 genome editing in murine ES cells. DSB repair pathway choice was determined using the IDAA system in the presence of 0.5mM 3DZnep. (A) HDR efficiency, (B) NHEJ efficiency, (C) HDR/NHEJ ratio, (D) total editing efficiency ($n = 5$ mean with standard deviation; t -test; *: $p \leq 0.05$; **: $p \leq 0.01$; ***: $p \leq 0.001$; ****: $p \leq 0.0001$; ns: $p > 0.05$).

3.3. 3DZnep promotes HDR in most cell lines tested

Next, we investigated whether 3DZnep showed cell type specific effects on genome editing. To this end we used the sgRNAs tested already in HEK293T cells on human U2OS cells and different sgRNAs targeting mouse gene orthologues in murine N2A neuroblastoma cells and embryonic stem (mES) cells. 3DZnep increased HDR for all genes tested in U2OS and mES cells by up to 80%. (Figs. 3, 4). In N2A cells, however, 3 of 5 genes showed a reduced HDR efficiency in the presence of 3DZnep and only 1 a significant increase (Fig. 5).

To further investigate the significance of the observed changes, we used the averages of the fold changes in HDR efficiency and total editing for the four 3DZnep treated cell lines (HEK293T, U2OS, mES, N2A) on the five different target genes (HOXD13, LPXN, PAX2, PHOX2B, TSPAN12; $n = 18$) and performed a statistical analysis. In this data set,

3DZnep induced a 1.33 \pm 0.41-fold increase in HDR that was highly significant in Student's t -test ($p = 0.00186$) (Suppl. Fig. 6). This very high significance strongly supports the pharmacological activity of 3DZnep on HDR genome editing efficiency. Total editing efficiency, on the other hand, was not significantly altered with an average fold-change of 1.002 \pm 0.036 ($p = 0.846$).

These data suggest that 3DZnep mainly skews the DNA repair pathway choice between HDR and NHEJ towards HDR, while cell type and gene specific differences exist.

3.4. 3DZnep increases off-target efficiency

To test the effect of 3DZnep on off-target efficiency in HEK293T cells, we used sgRNAs against *EMX1* and *VEGFA* described earlier [16,17] (Fig. 6A, C). Transfected cells were enriched by puromycin treatment. For both sgRNAs, 3DZnep treatment increased the off-target efficiency significantly (Fig. 6B, D). This resulted in a 26–30% increase of the off-target to on-target ratio. These data suggest that editing efficiency at off-target sites is elevated in the presence of 3DZnep.

3.5. 3DZnep effect on DSB repair pathway choice is independent of H3K27 methylation

3DZnep is described to inhibit histone methylation, and we confirmed reduced levels of H3K27me3, and H3K9me2, but not of H3K4me2 in response to 3DZnep in HEK293T cells (Supp. Fig. 7). However, neither inhibition or KO of the methyltransferase for H3K27me3 in HEK293T cells (Fig. 7) nor treatment of HEK293/TLR with inhibitors of H3K9 dimethylation (Fig. 1) increased HDR efficiency. Moreover, 3DZnep increased HDR efficiency also in the presence of inhibitors for H3K27me3. Interestingly, KO of EZH2 but not acute treatment with EZH2 inhibitors strongly reduced HDR/NHEJ ratio without affecting total editing efficiency. These data suggest that 3DZnep is altering HDR efficiency independent of the H3K27, H3K9, and H3K4 methylation.

3.6. 3DZnep treatment does not alter the expression of genes associated with DSB

To assess whether treatment with 3DZnep altered genome editing efficiency by changing expression of DNA repair relevant genes in HEK293T or mES cells, RNAseq analysis was performed. 1173 genes in HEK293T and 1411 genes in mES cells were significantly altered more than 2-fold, but none of the genes annotated to DSB repair were similarly altered (Supp. Table 4A) and none of the 23 similarly altered genes showed an obvious link to increased HDR efficiency based on published data (Supp. Table 4B). These data indicate high cell type specific effects of 3DZnep on transcription, but do not suggest that the HDR promoting effect of 3DZnep is caused by changes in mRNA levels.

3.7. 3DZnep might affect DSB repair by altering cell cycle

Earlier it was shown that increased length of S and G2 phases of the cell cycle can promote HDR efficiency [22]. Therefore, we assessed whether 3DZnep prolongs these cell cycle phases. HEK293T, U2OS, and N2A cells showed a reduction of G1 and an increase of S phase (Fig. 8). These changes were significant in HEK293T and N2A. The U2OS data were not significantly different by ANOVA analysis ($p(G1)$: 0.31; $p(S)$: 0.12; $p(G2)$: 0.88). However, while G2 was not changed in HEK293T and U2OS, it was significantly decreased in N2A. mES cells, in contrast, showed a massive increase of G2 and a decrease of G1 and S. While 3DZnep induced in all 4 cell lines tested an increase in S + G2 (Fold change in HEK293: 1,03; U2OS: 1,07; mES: 1,07; N2A: 1,08) compared to DMSO treated controls, this did not correlate well with the observed alterations in HDR efficiency, which increased most strongly in mES (1,71 fold over 3 genes tested), but was even slightly decreased in N2A (0,94 fold over 5 genes tested).

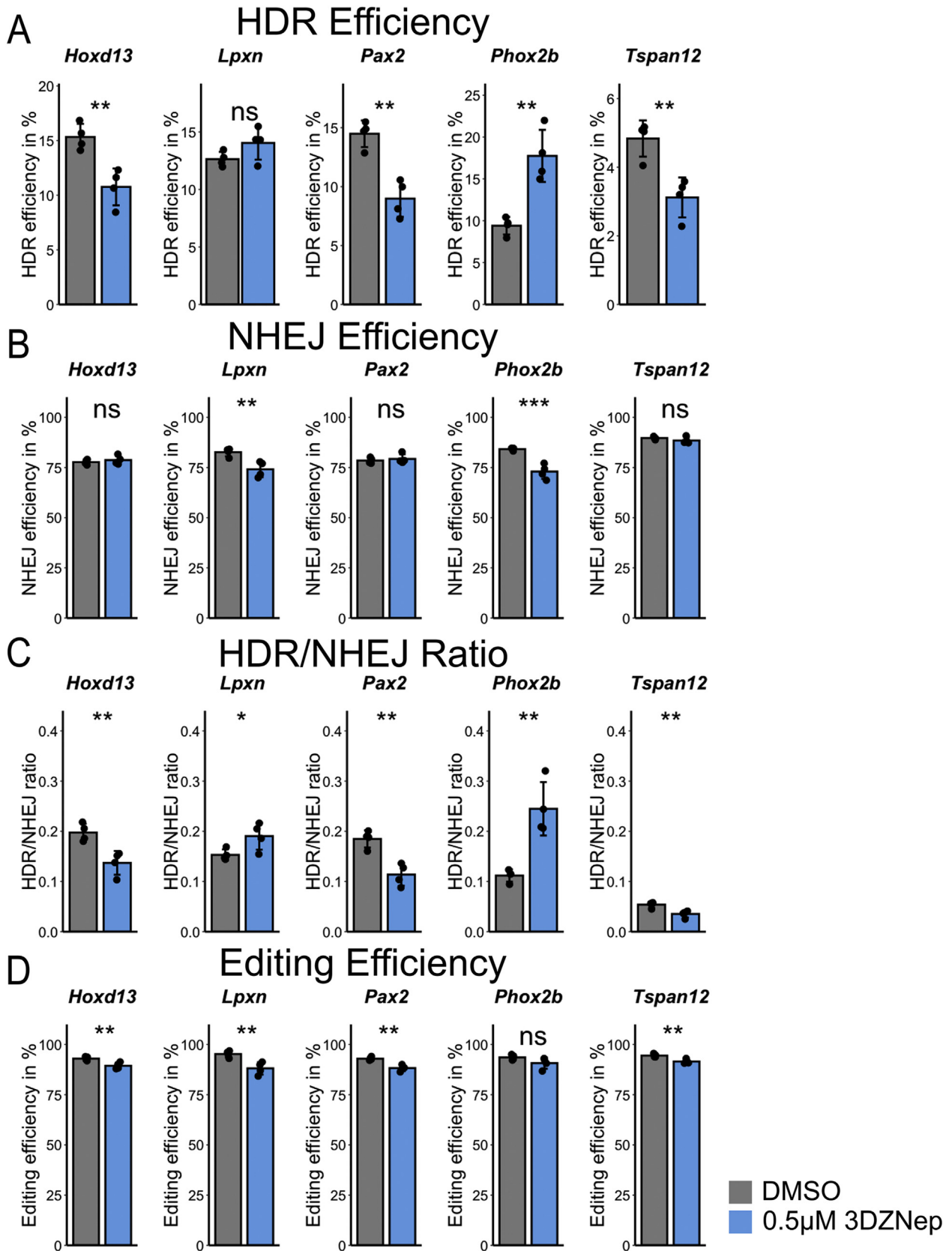


Fig. 5. 3DZnep influences pathway choice in CRISPR-Cas9 genome editing in murine N2A cells in a target specific manner. DSB repair pathway choice was determined using the IDAA system in the presence of 0.5mM 3DZnep. (A) HDR efficiency, (B) NHEJ efficiency, (C) HDR/NHEJ ratio, (D) total editing efficiency ($n = 4$; mean with standard deviation; t -test; * : $p \leq 0.05$; ** : $p \leq 0.01$; *** : $p \leq 0.001$; ns : $p > 0.05$).

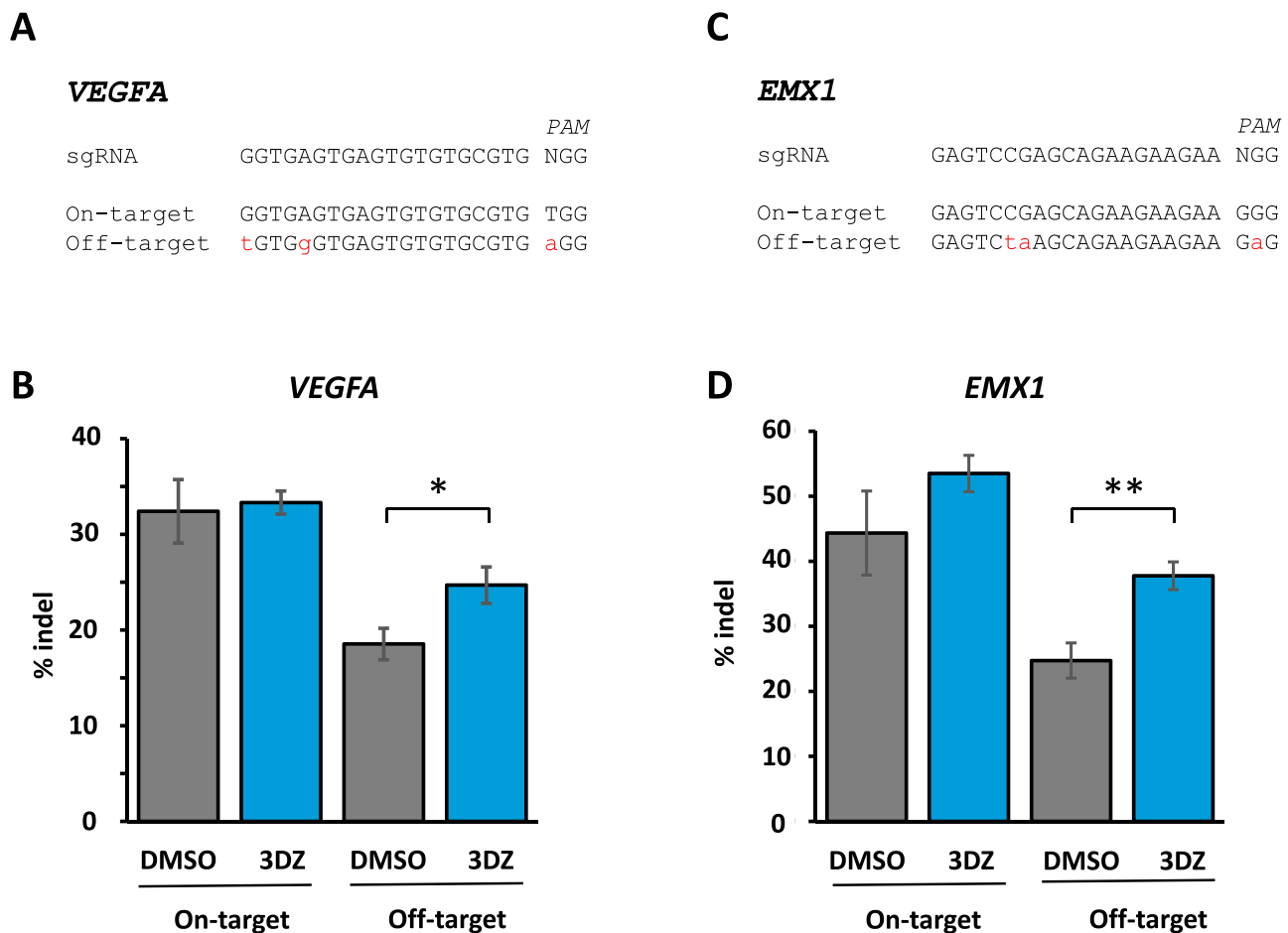


Fig. 6. 3DZNep increases off target efficiency in HEK293T cells. DSB repair efficiency was determined in the presence of 0.5mM 3DZNep (3DZ) or DMSO by Sanger sequencing and TIDE analysis. (A) sgRNA, on- and off-target sequence of *VEGFA*; (B) Genome editing efficiency of *VEGF* sgRNA; (C) sgRNA, on- and off-target sequence of *EMX1*. (D) Genome editing efficiency of *EMX1* sgRNA ($n = 3$; mean with standard deviation; t -test; * : $p \leq 0.05$; ** : $p \leq 0.01$).

These results suggest that the 3DZNep induced increase in HDR efficiency is partially mediated by an increased frequency of S and G2 cells, but that other positive (mES) as well as negative (N2A) mechanisms contribute as well.

4. Discussion

Chromatin modifications have been reported earlier to affect the efficiency of CRISPR-Cas9 genome editing [2–9]. Our study strongly supports this notion, but suggests in addition that downregulation of specific chromatin marks has effects on DSB repair that can depend significantly on the duration of the reduction before genome editing. While acute inhibition of H3K27me3 by EZH2 inhibitors showed no effect on CRISPR-Cas9 genome editing efficiency, permanent inhibition by EZH2 KO strongly decreased HDR efficiency without altering total editing efficiency. Investigating the effect of small molecules altering chromatin modification, it might therefore be useful to include different pre-incubation times before transfection of CRISPR-Cas9 to reveal long-term effects of chromatin modification. Interestingly, the H3K27 demethylase inhibitor GSK-J4 showed no antagonistic effect to EZH2 KO and strongly decreased both HDR and NHEJ, although the corresponding cell types were not exactly the same (HEK293 vs HEK293T).

A strong increase of the HDR to NHEJ ratio was found for high concentrations of the DNA methylation inhibitor 5-aza and the histone acetyltransferase inhibitor C646. However, these inhibitors also strongly reduced HDR efficiency, suggesting that they are important for both genome editing efficiency and repair pathway choice. Interestingly, the

histone deacetylation inhibitor TSA did not improve HDR or NHEJ under the conditions tested in contrast to the expectations [9]. These results indicate that regulation of CRISPR-Cas9 genome editing by chromatin modifications is highly dependent on concentration and timing of the inhibitors.

The only inhibitor which showed a significantly increased HDR efficiency in the fluorescent reporter system was 3DZNep. Validation studies on different target genes and different cell lines confirmed the HDR promoting effect of 3DZNep, which mostly resulted in a corresponding decrease in NHEJ, suggesting that 3DZNep affects the repair pathway choice, but not total editing efficiency. Introduction of an on-target DSB by sgRNA/Cas9 is therefore not strongly affected by 3DZNep. Furthermore, we did not see a dependency of HDR promotion of 3DZNep on the total level of genome editing or on the expression level of the target gene. Interestingly, however, 3DZNep promoted off-target genome editing in two genes tested, suggesting that off-target cutting efficiency followed by NHEJ repair is increased. This indicates that 3DZNep is controlling different molecular aspects of DSB DNA repair.

HDR is taking place in the S and G2 phase of the cell cycle and increasing the fraction of cells in these cell cycle phases had been shown to facilitate HDR over NHEJ during CRISPR genome editing [27]. 3DZNep treatment induced such a shift in the cell cycle, but we did not observe a strong correlation between the percentage of cells in S and G2 and the increase of HDR in the four cell lines tested. In N2A cells, the increase in S/G2 corresponded even to a slight reduction of HDR efficiency. Thus, 3DZNep affects DSB repair by different molecular mechanisms, of which one is the alteration of cell cycle distribution. Additional positive (mES)

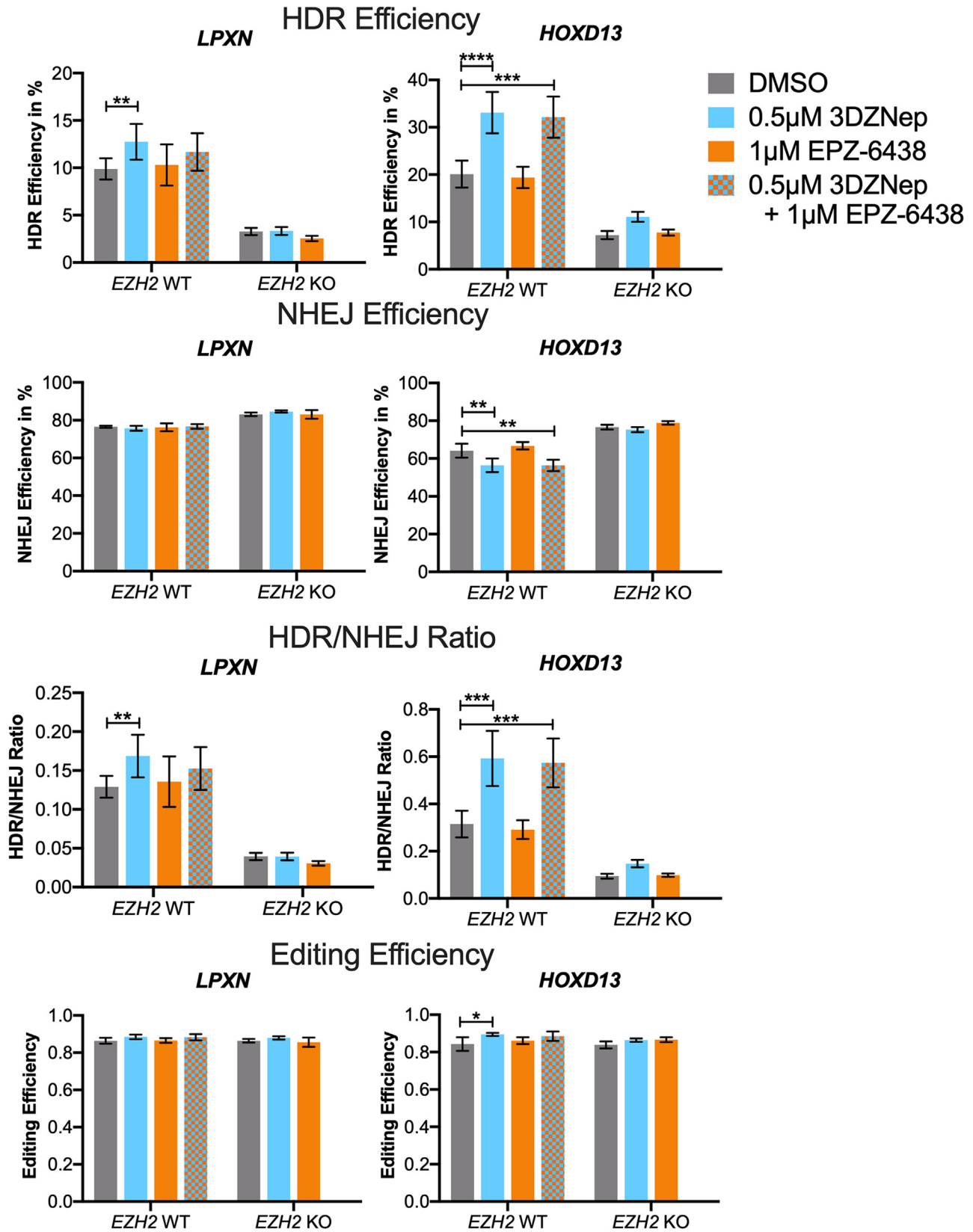


Fig. 7. 3DZNep effect on CRISPR-Cas9 genome editing is independent of H3K27me3. CRISPR-Cas9 genome editing of *HOXD13* and *LPXN* was carried out in WT and EZH2 KO HEK293T cells treated with the indicated inhibitors. DSB repair pathway choice was determined using the IDAA system ($n \geq 3$; mean with standard deviation; ANOVA; *: $p \leq 0.05$; **: $p \leq 0.01$; ***: $p \leq 0.001$; ****: $p \leq 0.0001$).

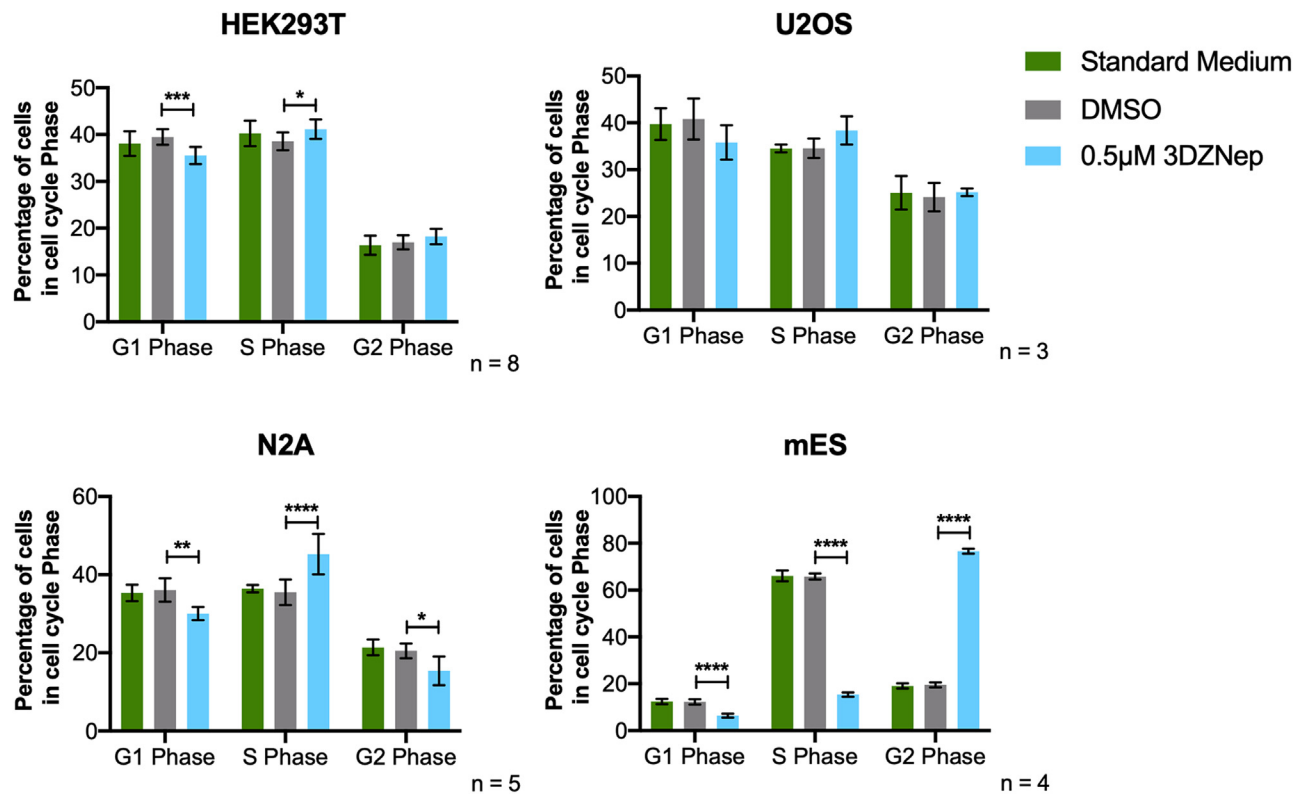


Fig. 8. 3DZNep induces increased S and G2 phases of the cell cycle. Cell cycle analysis of HEK293T, U2OS, N2A or mES cells treated with 3DZNep, DMSO, or standard medium. HEK293T and N2A cells were analyzed by PI staining. For U2OS and mES cells staining with PI and EdU was evaluated (Mean with standard deviation; two-way ANOVA; * p-value ≤ 0.05 ; ** p-value ≤ 0.01 ; *** p-value ≤ 0.001 ; **** p-value ≤ 0.0001).

and negative (N2A) effects appear to contribute in a cell type specific manner.

Since no alterations in the expression of DNA repair genes could be found in two 3DZNep treated cell lines, 3DZNep is conceivably acting by a posttranscriptional mechanism such as protein methylation. The best described target, H3K27me3, however, appears not to be involved as acute, specific inhibition of this pathway did not promote HDR and did not interfere with the effect of 3DZNep. Instead, it is possible that 3DZNep inhibits the methylation of HDR regulating molecules by its activity as an efficient S-adenosyl-homocysteine hydrolase inhibitor. Indeed, inhibition of S-adenosyl-homocysteine hydrolase was reported to block cellular methylation not only of proteins, but also of phospholipids, small molecules, DNA, and RNA [28]. The cellular effects of 3DZNep are therefore most likely complex and it is well conceivable that it affects CRISPR-Cas9 genome editing efficiency by different pathways. Future studies could explore the effects of 3DZNep on cellular methylation, which might guide further improvement of the technology.

5. Conclusions

3DZNep is a novel promoter of HDR pathway choice in CRISPR-Cas9 genome editing with little target gene specificity, which is applicable in different cell lines including mES cells.

Competing interest statement

The authors declare the following competing interests: N.B. works as a consultant with direct customer contact for Körber Pharma Software GmbH, a manufacturing execution system (MES) / electronic batch record (EBR) provider supporting the GMP regulated production of pharmaceutical industries including AstraZeneca and Novo Nordisk. M.M. is an employee and shareholder of AstraZeneca. S.W. is an industrial PhD student at AstraZeneca. E.P.B. is an employee at Novo Nordisk.

K.H. is a co-founder of Dania Therapeutics, consultant for Inthera Bioscience AG and a scientific advisor for MetaboMed Inc and Hannibal Innovation. All other authors declare no competing interests.

Funding statement

This project has received funding from the European Union's Horizon 2020 research and innovation program under the Marie Skłodowska-Curie grant agreement No 765269.

Supp. Table 1: A: Guide sequences used for design of sgRNA with PAM shown in italics. B: ssODN used for HDR of human and murine target genes. Shown in italics is the 8 bp introduction during HDR repair, with the HindIII restriction site underlined. C: Primers used for PCR with overhangs indicated in italics and 8 bp introduction to mimic HDR shown as underlined.

Supp. Table 2: Inhibitors tested for alteration of HDR and NHEJ.

Supp. Table 3: Mean expression level of target genes in HEK293T cells as determined by RNAseq after treatment with 3DZNep or DMSO.

Supp. Table 4: A: Repair genes with significantly and more than two-fold altered expression after 3DZNep treatment in HEK293T (top) or mES (bottom) cells. p-values estimated with the Wald test and adjusted with the Benjamini-Hochberg procedure. $n = 3$ biological replicates for either cell line.

B: Genes with a similar change of expression after 3DZNep treatment in HEK293T and mES cells. FC = Fold Change, Adj(p) = adjusted p-value.

Suppl. Fig. 1: The Traffic Light Reporter System. (A) The traffic light reporter (TLR) expressed in HEK293T contains two non-functional fluorescent markers expressed under a CAG promoter and fused by a T2A cleavage site. A DSB introduced in the non-functional Venus sequence can be repaired by HDR or NHEJ. HDR repair, exploiting the donor plasmid, results in intact Venus expression. A frameshift mutation of 2 bp leads to in-frame expression of RFP, detecting a fraction of

cells that have undergone NHEJ (Modified after [18]). B) HEK293/TLR cells were seeded and 24 h later transfected with a sgRNA/BFP expression plasmid and a donor plasmid to restore Venus expression via HDR. At the time of transfection, 48 h inhibitor treatment was started. FACS analysis quantified the numbers of cells that have undergone HDR (Venus) or NHEJ (TagRFP) within the positively transfected (BFP) cell population.

Suppl. Fig. 2: Evaluation of genome editing efficiency by ssODN dependent CRISPR genome editing. (A) Restriction digest. Genomic PCRs are run with primers spanning the *PAX2* target site. A HindIII restriction site inserted during HDR repair is detected by restriction digest. Restriction digests run on PCR amplicons from non-edited cells result in only one band at 760 bp. The same assay run on PCR amplicons from a modified cell pool results in three bands. The bands at 279 bp and 481 bp represent HDR events. B) NGS. Sample preparation for NGS included several rounds of PCR, creating PCR fragments (shown in yellow) clearly labelled with barcodes (shown in different colors). Different samples were then pooled and sequenced. Introduction of the 8 bp insert by HDR (shown in purple) at the *PAX2* locus was detected by the exact nucleotide string (highlighted in the box). Sequences will be quantitatively analyzed by the RIMA software. C) TIDE/TIDER. Shown is an example for DSB evaluation at the *PAX2* locus with HDR resulting in an 8 bp insertion. Genomic PCR covering the edited site is Sanger sequenced. In addition, Sanger sequencing files representing unedited cells (WT control sample) or 100% HDR edited cells (HDR Reference Sample) are required. All three Sanger sequencing files are uploaded to a free web-interface. The TIDER software estimates HDR and NHEJ efficiencies by quantification of relative peak heights. TIDE is a version distinguishing only modified or not modified sequences. D) ICE. Experimental procedure is similar to evaluation by TIDER. The main difference is that no HDR Reference Sample Sanger sequencing file is required. The HDR sequence is typed in manually by the user. E) IDAA. Genomic DNA is extracted from edited cells and a tri-primer PCR run. Amplification of the *PAX2* locus leads to a PCR product of 372 bp for WT cells and 380 bp for cells that have undergone HDR repair, and different sizes for NHEJ events. Running fragments on a sequenator allows quantified analysis at single nucleotide resolution.

Suppl. Fig. 3: Increase in HDR editing of *PAX2* gene after 3DZNep treatment of HEK293T cells confirmed by different readouts. Cells were treated with 0.5 μM 3DZNep or an equivalent amount of DMSO for 48 h starting at transfection. Positively transfected cells were selected with 2 $\mu\text{g}/\text{ml}$ puromycin over 4 days. Genomic DNA was used for HDR evaluation by restriction digest, NGS, TIDER, ICE OR IDAA. Absolute HDR efficiency: Fraction of mutated reads in mapped reads; Relative HDR efficiency: Fraction of mutated reads in mutated mapped reads ($n = 3$; mean with standard deviation; t -test; * : $p \leq 0.05$; ** : $p \leq 0.01$)

Suppl. Fig. 4: 3DZNep does not alter the mutational profile of CRISPR-Cas9 genome editing in HEK293T cells. CRISPR-Cas9 genome editing was carried out in the presence or absence of 0.5mM 3DZNep and analyzed for amplicon length by IDAA. WT peaks are highlighted in yellow, HDR peaks are at +8 bp.

Suppl. Fig. 5: 3DZNep reduces both c-NHEJ and c-MMEJ editing of the *PAX2* gene in HEK293T cells. Bar graphs show the mean efficiencies of different repair events of RIMA analyzed NGS data of HEK293T cells mutated at the *PAX2* gene. Cells were treated with 0.5 μM 3DZNep or an equivalent amount of DMSO for 48 h starting at transfection. Positively transfected cells were selected with 2 $\mu\text{g}/\text{ml}$ puromycin over 4 days. Absolute editing efficiency: Fraction of mutated reads in mapped reads; HDR: Efficiency of ssDNA donor integration; c-MMEJ: ≥ 2 bp deletions surrounded by microhomologies; other-EJ: All other mutations which are not classified as c-MMEJ or HDR; 1 bp NHEJ: 1 bp insertions or deletion, which are most likely c-NHEJ mediated.

Suppl. Fig. 6: 3DZNep promotes HDR across 4 cell lines and 5 genes, but not total gene editing. Presented are the average values for HDR efficiency and total editing efficiency for 4 cell lines and 5 target genes as shown in Figs. 2–5, and the statistical analysis ($n = 18$)

Suppl. Fig. 7: Effect of 3DZNep treatment on H3K27me3, H3K9me2, and H3K4me2 in HEK293T cells.

3DZNep treatment significantly decreased H3K27me3 and H3K9me2, but not H3K4me2 in HEK293T cells ($n = 3$; mean with standard deviation; t -test; ** : $p \leq 0.01$; *** : $p \leq 0.001$; **** : $p \leq 0.0001$; ns : $p > 0.05$).

Declaration of Competing Interest

The authors declare the following financial interests/personal relationships which may be considered as potential competing interests.

Data availability

Data will be made available on request.

Acknowledgments

For help with experiments we thank Claire Katrine Beier Holden, Camilla Andersen, Jonas Westergaard Højfeldt, Minyan Li, Anna Fossum and Rajesh Somasundaram.

Supplementary materials

Supplementary material associated with this article can be found, in the online version, at doi:10.1016/j.ggedit.2022.100023.

References

- [1] Bischoff N, Wimberger S, Maresca M, et al. Improving precise CRISPR genome editing by small molecules: is there a magic potion? *Cells* 2020;9:1318. doi:10.3390/jms22010207.
- [2] Cuzzo C, Porcellini A, Angrisano T, et al. DNA damage, homology-directed repair, and DNA methylation. *PLoS Genet* 2007;3:e110. doi:10.1371/journal.pgen.0030110.
- [3] Pfister SX, Ahrabi S, Zalmas LP, et al. SETD2-dependent histone H3K36 trimethylation is required for homologous recombination repair and genome stability. *Cell Rep* 2014;7:2006–18. doi:10.1016/j.celrep.2014.05.026.
- [4] Pai CC, Deegan RS, Subramanian L, et al. A histone H3K36 chromatin switch coordinates DNA double-strand break repair pathway choice. *Nat Commun* 2014;5:4091. doi:10.1038/ncomms5091.
- [5] Kallimasioti-Pazi EM, Thelakkad Chathoth K, Taylor GC, et al. Heterochromatin delays CRISPR-Cas9 mutagenesis but does not influence the outcome of mutagenic DNA repair. *PLoS Biol* 2018;16:e2005595. doi:10.1371/journal.pbio.2005595.
- [6] Janssen JM, Chen X, Liu J, Gonçalves MAFV. The chromatin structure of CRISPR-Cas9 target DNA controls the balance between mutagenic and homology-directed gene-editing events. *Mol Ther Nucleic Acids* 2019;16:141–54. doi:10.1016/j.omtn.2019.02.009.
- [7] Sulkowski PL, Oeck S, Dow J, et al. Oncometabolites suppress DNA repair by disrupting local chromatin signalling. *Nature* 2020;582:586–91. doi:10.1038/s41586-020-2363-0.
- [8] Bromberg KD, Mitchell TR, Upadhyay AK, et al. The SUV4-20 inhibitor A-196 verifies a role for epigenetics in genomic integrity. *Nat Chem Biol* 2017;13:317–24. doi:10.1038/nchembio.2282.
- [9] Li G, Zhang X, Wang H, et al. Increasing CRISPR/Cas9-mediated homology-directed DNA repair by histone deacetylase inhibitors. *Int J Biochem Cell Biol* 2020;125:105790. doi:10.1016/j.biocel.2020.105790.
- [10] Glazer RI, Knode MC, Tseng CK, et al. 3-Deazaneplanocin A: a new inhibitor of S-adenosylhomocysteine synthesis and its effects in human colon carcinoma cells. *Biochem Pharmacol* 1986;35:4523–7. doi:10.1016/0006-2952(86)90774-4.
- [11] Fiskus W, Wang Y, Sreekumar A, et al. Combined epigenetic therapy with the histone methyltransferase EZH2 inhibitor 3-deazaneplanocin A and the histone deacetylase inhibitor panobinostat against human AML cells. *Blood* 2009;114:2733–43. doi:10.1182/blood-2009-03-213496.
- [12] Højfeldt JW, Hedehus L, Laugesen A, et al. Non-core subunits of the PRC2 complex are collectively required for its target-site specificity. *Mol Cell* 2019;76:423–36 e3. doi:10.1016/j.molcel.2019.07.031.
- [13] Müller I, Moroni AS, Shlyueva D, et al. MPP8 is essential for sustaining self-renewal of ground-state pluripotent stem cells. *Nat Commun* 2021;12:3034. doi:10.1038/s41467-021-23308-4.
- [14] Ye J, Coulouris G, Zaretskaya I, et al. Primer-BLAST: a tool to design target-specific primers for polymerase chain reaction. *BMC Bioinf* 2012;13:134. doi:10.1186/1471-2105-13-134.
- [15] Concordet JP, Haeussler M. CRISPOR: intuitive guide selection for CRISPR/Cas9 genome editing experiments and screens. *Nucleic Acids Res* 2018;46(W1):W242–5. doi:10.1093/nar/gky354.
- [16] Gee P, Lung MSY, Okuzaki Y, et al. Extracellular nanovesicles for packaging of CRISPR-Cas9 protein and sgRNA to induce therapeutic exon skipping. *Nat Commun* 2020;11:1334. doi:10.1038/s41467-020-14957-y.

- [17] Fu Y, Foden JA, Khayter C, et al. High-frequency off-target mutagenesis induced by CRISPR-Cas nucleases in human cells. *Nat Biotechnol* 2013;31:822–6. doi:10.1038/nbt.2623.
- [18] Chu VT, Weber T, Wefers B, et al. Increasing the efficiency of homology-directed repair for CRISPR-Cas9-induced precise gene editing in mammalian cells. *Nat Biotechnol* 2015;33:543–8. doi:10.1038/nbt.3198.
- [19] Lonowski LA, Narimatsu Y, Riaz A, et al. Genome editing using FACS enrichment of nuclease-expressing cells and indel detection by amplicon analysis. *Nat Protoc* 2017;12:581–603. doi:10.1038/nprot.2016.165.
- [20] Lundin A, Porritt MJ, Jaiswal H, et al. Development of an ObLiGaRe doxycycline inducible Cas9 system for pre-clinical cancer drug discovery. *Nat Commun* 2020;11:4903. doi:10.1038/s41467-020-18548-9.
- [21] Taheri-Ghahfarokhi A, Taylor BJM, Nitsch R, et al. Decoding non-random mutational signatures at Cas9 targeted sites. *Nucleic Acids Res* 2018;46:8417–34. doi:10.1093/nar/gky653.
- [22] Brinkman EK, van Steensel B. Rapid quantitative evaluation of CRISPR genome editing by TIDE and TIDER. *Methods Mol Biol* 2019;1961:29–44. doi:10.1007/978-1-4939-9170-9_3.
- [23] Zhao Y, Chung MC, Konate MM, et al. PM, FPKM, or normalized counts? A comparative study of quantification measures for the analysis of RNA-seq data from the NCI patient-derived models repository. *J Transl Med* 2021;19:269. doi:10.1186/s12967-021-02936-w.
- [24] Huang da W, Sherman BT, Lempicki RA. Systematic and integrative analysis of large gene lists using DAVID bioinformatics resources. *Nat Protoc* 2009;4:44–57. doi:10.1038/nprot.2008.211.
- [25] Sansbury BM, Wagner AM, Nitzan E, et al. CRISPR-directed *in vitro* gene editing of plasmid DNA catalyzed by Cpf1 (Cas12a) nuclease and a mammalian cell-free extract. *CRISPR J* 2018;1:191–202. doi:10.1089/crispr.2018.0006.
- [26] Bloh K, Rivera-Torres I, N. A consensus model of homology-directed repair initiated by CRISPR/cas activity. *J Mol Sci* 2021;22:3834. doi:10.3390/ijms22083834.
- [27] Lin S, Staahl BT, Alla RK, Doudna JA. Enhanced homology-directed human genome engineering by controlled timing of CRISPR/Cas9 delivery. *Elife* 2014;3:e04766. doi:10.7554/eLife.04766.
- [28] Chiang a PK. Biological effects of inhibitors of S-adenosylhomocysteine hydrolase. *Pharmacol Ther* 1998;77:115–34.